On the Mode-Coupling Formation of Complex Modes in a Nonreciprocal Finline

Ching-Kuang C. Tzuang, *Senior Member, IEEE* and Jinq-Min Lin, *Student Member, IEEE*

Abstract—**This paper studies and models the mechanism for forming the complex modes commonly found in boxed quasi-planar or planar guided-wave structures. To illustrate the fact that the mode-coupling among the various forms of modes is closely related to the formation of complex modes, the dispersion characteristics of the complex propagation constants (or the so-called mode spectrum) of a nonreciprocal unilateral finline are obtained by the rigorous full-wave SDA (spectral-domain approach). It is found that in the mode spectrum of the nonreciprocal finline, a forward wave and a backward wave interact to produce a pair of complex modes. The interactions between two forward (backward) traveling waves, between a forward wave and a backward wave, and between two complex waves (modes) are modeled by applying the model-coupling theory. The concept of hypothetical modes is introduced in the model. These hypothetical modes are obtained by applying mode-coupling theory to the mode spectrum previously obtained. The approximate values obtained for the propagation constants of the three types of wave interactions using the model presented in the paper are in close agreement with those given by the full-wave SDA.**

I. Introduction

IN *open* lossless media, the following types of guided complex waves at a plane interface have been reported [1]: 1) a forward surface wave and a backward surface wave coexisting in pairs and carrying no net real power, 2) two degenerate proper (spectral) complex waves coupled in a manner that no real power is carried, and 3) improper leaky waves. The existence of complex waves (modes) in electrically *shielded* lossless waveguides, e.g., dielectric-loaded partially filled circular waveguide [2], double-layer circular waveguide [3], [4], shielded dielectric image guide [5], [6], finline [7], microstrip line [8], [9], suspended coupled microstrip line [10], CPW (coplanar waveguide) [11], and asymmetric coupled suspended striplines [12], has already been reported. These complex modes, it has been shown, appear inside an electric enclosure and they are not leaky waves. The complex modes are also physical modes which must be considered if accurate results are to be obtained for a discontinuity problem. Omar and Schünemann demonstrated this in their analysis of a finline step discontinuity problem [7]. The complex modes are therefore the essential constituent part of the mode spectrum associated with many inhomogeneously filled waveguides.

Manuscript received May 13, 1992; revised December 14, 1992. This work was supported in part by the Taiwan National Science Council under Grant NSC 82-0404-E-009-194 and in part by CS82-0210-D006-26.

C.-K. C. Tzuang is with the Institute of Communication Engineering and MIRSC (Microelectronic and Information System Research Center), National Chiao Tung University, No. 1001, Ta Hsueh Road, Hsinchu, Taiwan, Republic of China.

J.-M. Lin is with the Institute of Electronics, National Chiao Tung University, and ERSO (Electronics Research & Service Organization), Hsinchu, Taiwan, Republic of China.

IEEE Log Number 9210214.

Some research has been conducted toward understanding the general properties of the guided complex modes. Omar and Schünemann show that complex modes and backward waves can be supported by inhomogeneously filled and anisotropically filled lossless waveguides of arbitrarily shaped cross section [13]. Another comprehensive treatment on the existence of complex modes in such lossless inhomogeneously filled dielectric waveguides has been reported separately by Mrozowski and Mazur [14]–[16]. They showed that, in slightly perturbed homogeneous structures, a pair of degenerate TE and TM modes existing in the homogeneous guide are quite sensitive to the small perturbation. These degenerate and below-cutoff modes then lead to the formation of complex modes in pairs. Subsequently, they established a formulation that predicts the existence of complex modes in lossless dielectric guides [15], [16].

The main aim of this paper is to understand and model in a very general sense the mechanism which forms the complex modes. Apart from presenting an analysis of the complex modes in the reciprocal waveguides, this paper gives the dispersion characteristics of the propagation constants, or the so-called mode spectrum, of a *nonreciprocal* unilateral finline calculated by the rigorous full-wave SDA (spectral-domain approach). Propagation in a nonreciprocal waveguide consists of a group of forward traveling waves and a group of backward traveling waves, of which the propagation constants *differ in sign and magnitude*. This allows us to plot the mode spectrum, as shown in Figs. 3–7 and discussed in Section IV, as a function of frequency. The dual vertical axes are centered at zero value. The left axis is for the normalized propagation constant (β/ko), while the right axis is for the normalized attenuation constant (α/ko). Such an arrangement for the plotting of mode spectrum of the nonreciprocal finline differs from all the above-mentioned reports for the reciprocal waveguides [2]–[16] and nonreciprocal waveguides [17]–[19]. In these reports, the normalized propagation constant is assumed to be only either positive or negative in value. Section IV summarizes three types of wave interactions depicted (in the mode spectrum), namely, 1) between a forward (backward) traveling wave and a forward (backward) traveling wave, 2) between a forward wave and a backward wave, and 3) between a pair of complex modes and a pair of complex modes.

These various types of wave interactions between different modes can be explained qualitatively by invoking the mode-coupling theory [20] in Section V. The theory is briefly reviewed and extended to explain how different types of mode interactions are established. Section VI introduces the concept of *hypothetical modes*, which are obtained by applying the mode-coupling theory to the mode spectrum previously obtained by the full-wave SDA. The hypothetical modes are assumed to be either linear or elliptical with frequency although they are not necessarily linear or elliptical. The mode couplings of these hypothetical modes result in propagation constants of which the values are in very close agreement with the full-wave data for the various types of mode interactions discussed in Sections IV and V. The procedure to determine the coupling coefficients between these various mode interactions and the corresponding hypothetical modes is presented in detail. The important conclusions are outlined in Section VII.

For the sake of clarity, Section II lists the symbols used throughout this paper. Section III states the problems associated with the complex modes.

II. List of Symbols

Throughout the paper, the lossless waveguide cross section is assumed to be in the Cartesian x-y plane. The waveguide supports modes propagating along the longitudinal z direction. We list the following symbols for reference.

$e^{j\omega t}$: the time-harmonic factor of angular frequency $\omega = 2\pi f$

$e^{-j\gamma z}$: the z-dependence factor

$\gamma = \beta - j\alpha$: γ is the complex propagation constant, β and α are real numbers

β: the propagation constant, or the real part of the complex propagation constant

α: the attenuation constant, or the imaginary part of the complex propagation constant

γ_p: the complex propagation constant of the hypothetical mode p

γ_q: the complex propagation constant of the hypothetical mode q

the forward traveling wave [20]: $\beta > 0$, $\alpha = 0$

the backward traveling wave [20]: $\beta < 0$, $\alpha = 0$

the forward wave [21]: $(\beta) \cdot (\partial\beta/\partial\omega) > 0$

the backward wave [21]: $(\beta) \cdot (\partial\beta/\partial\omega) < 0$

the group velocity $v_g = (\partial\beta/\partial\omega)^{-1}$

III. Statement of Problems Associated with Complex Modes

The time-harmonic solutions for the complex modes of a reciprocal waveguide are located in the four quadrants of the complex γ plane [4]. These complex modes (γ) which appear in pairs can be divided into two types. Omar and Schünemann, for example, chose one pair of the complex modes of the *first type* for their finline discontinuity analysis [7]

$$\gamma = \pm\beta - j\alpha \quad (\beta > 0, \alpha > 0) \quad \text{(pair 1 of the first type)}. \tag{1}$$

They also demonstrated that, by choosing pair 1 of the first type, the Poynting power of the complex modes carries no real (active) power. Since the finline is reciprocal, the second remaining choice for γ is

$$\gamma = \pm\beta + j\alpha \quad (\beta > 0, \alpha > 0) \quad \text{(pair 2 of the first type)}. \tag{2}$$

By investigating the derived characteristic equation for the normalized propagation constant of a reciprocal dielectric-loaded circular waveguide, Clarricoats reported that in the vicinity of the special points denoted by P, Q, R, S shown in Fig. 1, the magnitude and sign of the complex propagation constant γ (the complex modes) can be assigned as indicated [2]. No complex modes exist near points P and Q in case (a) and case (b) of Fig. 1. For case (c), the complex modes near point R can be grouped into two pairs according to equations (1) and (2). While for case (d), the complex modes near point S take the following forms:

$$\gamma = \beta \pm j\alpha \quad (\beta > 0, \alpha > 0) \quad \text{(pair 1 of the second type)} \tag{3}$$

or

$$\gamma = -\beta \pm j\alpha \quad (\beta > 0, \alpha > 0) \quad \text{(pair 2 of the second type)}. \tag{4}$$

The following questions can be posed.

1) How *general* is Clarricoats' theory? Can it be applied to guided-wave structures other than the special dielectric-loaded circular waveguide that he investigated?

2) Does a general theory exist that can explain and model what happens in the mode spectrum of Fig. 1 and that of all the above-mentioned papers [2]–[19]? For example, Clarricoats pointed out that, referring to the case (d), where a forward wave and a backward wave coexist, there must be a pair of complex modes. Case (c), however, generates a pair of complex modes not resulting from a forward wave and a backward wave.

3) When will the two propagating modes or the two evanescent modes *not* form the complex modes?

In what follows, we will report a unified theory to resolve the questions raised in this section.

IV. Complex Modes in a Nonreciprocal Finline

Equations (1)–(4) represent various possible ways of grouping the solutions for the complex modes in the γ-plane, at least for the special case studies conducted by Clarricoats, Omar and Schünemann, and others [2]–[19]. If a *nonreciprocal* waveguide can support complex modes, then, because of the clear distinction between a forward traveling wave ($\beta > 0$) and a backward traveling wave ($\beta < 0$) in this type of waveguide, only one pair of complex modes will be generated. The nonreciprocity destroys the possibility of choosing the second pair of complex modes once the first pair of complex modes is obtained. In contrast to the two-pair solutions for the complex

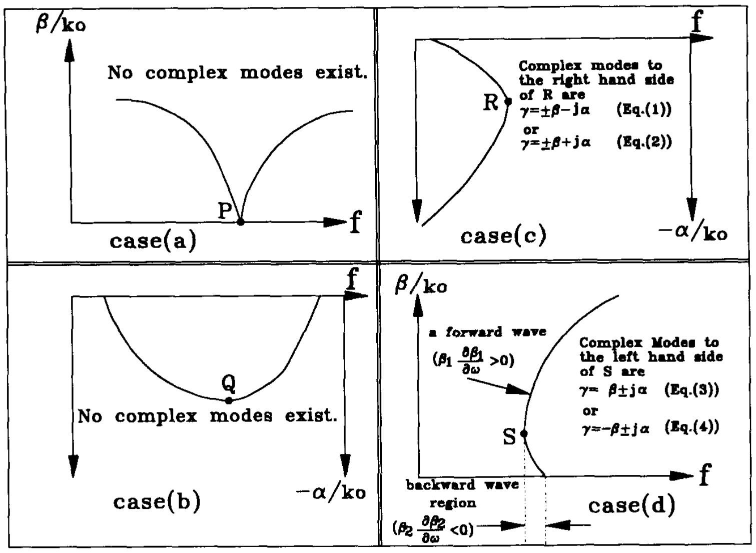

Fig. 1. Properties of the complex propagation constants near the special points denoted as P, Q, S for the four types of mode spectrum, case (a)-through-(d), respectively. Case (a) two degenerate cut-off modes at point P. Case (b) $\partial\alpha/\partial f = 0$ at point Q, the bottom of an ellipse shape. Case (c) $\partial\alpha/\partial f = \infty$ at point R, where the complex modes are in either $\pm\beta + j\alpha$ or $\pm\beta - j\alpha$ mathematical form. Case (d) $\partial\beta/\partial f = \infty$ at point S, where the complex modes are in either $\beta \pm j\alpha$ or $-\beta \pm j\alpha$ mathematical form.

modes in a reciprocal waveguide, the one-pair solutions for the complex modes in a nonreciprocal waveguide distribute themselves at only two of the four quadrants of the complex γ plane. Thus, the complexity of the mode spectrum containing the complex modes is reduced by half.

To illustrate the complex modes existing in a nonreciprocal waveguide, the mode spectrum (Ey-odd, Ex-even) of a symmetric unilateral finline with the material and structural parameters shown in Fig. 2 is plotted in Fig. 3. As reported in [22], the finline dispersion characteristics shown in Fig. 3 changed little when the applied dc magnetic field Ho varied from 500 Oe to 30 Oe. It is believed that Fig. 3 illustrates the common dispersion characteristics of an electrically shielded nonreciprocal waveguide. A ferrite substrate magnetized in the x-direction is sandwiched between two homogeneous dielectric layers with relative dielectric constants ε_2 and ε_4. Another homogeneous layer of ε_1 is to the right of the metal fins. Fig. 3 has dual vertical axes: on the left is the normalized propagation constant, whereas on the right is the normalized attenuation constant.

Being a nonreciprocal waveguide, the finline has many forward traveling waves which are denoted as F_1–F_7 in Fig. 3. These forward traveling waves, by definition, have positive real propagation constants ($\gamma > 0$). In contrast, B_1–B_7, which denote the backward traveling waves, have negative real propagation constants ($\gamma < 0$). These two groups of modes occupy the upper half and lower half of the mode spectrum, respectively. Three types of mode interactions which exist in the Fig. 3 will be discussed.

The first type of mode interaction is that the mode spectra, represented by F_1–F_7 (or B_1–B_7), neither intersect with each other, although some come close to each other, nor form any complex modes. For example, frame (a), at the upper side

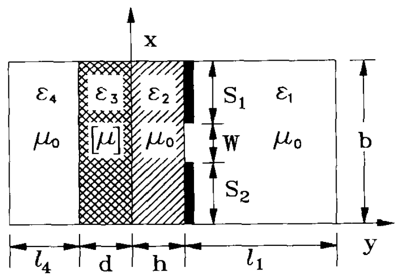

Fig. 2. Cross-sectional geometry of a unilateral finline integrated on the stratified layers containing a ferrite substrate magnetized in x-direction. The structural and material parameters are: $l_1 = 3.556$ mm, $d = h = 1$ mm, $l_4 = 1.556$ mm, $b = 3.556$ mm, $s_1 = s_2 = 1.628$ mm, $w = 0.3$ mm, $\varepsilon_1 = \varepsilon_4 = 1, \varepsilon_2 = \varepsilon_3 = 12.5, 4\pi Ms = 4900$G, and $H_o = 500$Oe.

of Fig. 3, shows that the modes designated as F_2 and F_3 have normalized propagation constants which differ by a very small value near 32.5 GHz. Similarly, in frame (b), the two backward traveling modes B_3 and B_4 do not intersect near 39.2 GHz.

The second type of implied mode interaction illustrated in Fig. 3 is the type shown by the modes designated as F_4–E_4, F_5–B_5, F_6–B_6 [frame (c)], and F_7–B_7 pairs. The F_7–B_7 pair, for example, constitutes a pair of complex modes below 41.3 GHz, where $\partial\beta/\partial\omega = \infty$. A detailed SDA study of the F_7–B_7 pair indicates that at the point where the group velocity is zero, i.e., $(\partial\beta/\partial\omega)^{-1} = 0$ (or $\partial\beta/\partial\omega = \infty$). Therefore, a small backward wave region exists in Fig. 3. This will be discussed in more detail in Section V. All the F_i–B_i pairs, $i = 4$ to 7, have small backward regions. The complex modes exist to the left of the intersect points where $\partial\beta_i/\partial\omega = \infty$ and $i = 4$ to 7. These complex modes are found to be of either $\gamma = \beta \pm j\alpha$ type [equation (3)] or $\gamma = -\beta \pm j\alpha$ [equation (4)]

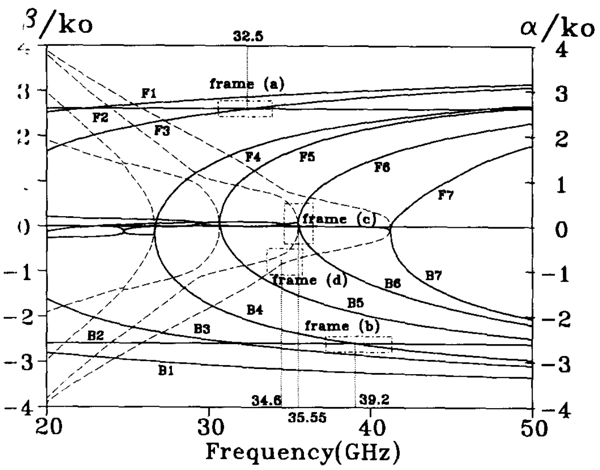

Fig. 3. The mode spectrum (Ex-even, Ey-odd) of a symmetric unilateral finline of Fig. 2. The solid lines represent the normalized propagation constant (the real part of the complex propagation constant) and correspond to the left hand side of vertical axis. The dashed lines represent the normalized attenuation constant (the imaginary part of the complex propagation constant) and correspond to the right hand side of vertical axis.

type. These types of complex modes coincide with the case (d) of Fig. 1, where complex modes coexist with the backward waves and the complex modes possess the mathematical form of either equation (3) or (4). The complex modes found here are apparently the result of mode interaction of a forward wave and a backward wave.

The third mode interaction is not merely confined to the modes possessing real propagation constants, but may occur between two complex modes. This additional complication is shown in frame (d) of Fig. 3. In order to understand why the imaginary parts do not intersect and real parts do, the real and imaginary parts of the propagation constant need to be investigated simultaneously. Similar observations are found in other locations of Fig. 3.

In summary, when two modes with nearly equal propagation constants interact, the result of mode interaction is either modes with purely real propagation constants or modes with complex propagation constants (complex modes). Furthermore, the various types of complex modes may also interact to produce other complex modes.

In the next section, the mode-coupling theory will be reviewed. This theory can be used to explain all the above-mentioned observations on the mode spectrum of Fig. 3 qualitatively and to model the various types of the mode interactions quantitatively.

V. Mode-Coupling Theory and the Complex Modes

A. *Review of Mode-Coupling Theory*

When two independent modes γ_p and γ_q propagate along separate waveguides and couple through an aperture, the resultant modal solutions after coupling has occurred are designated as γ_1 and γ_2. Pierce formulated the relationship between (γ_1, γ_2) and (γ_p, γ_q) as follows [20]:

$$\gamma_1 = \frac{\gamma_p + \gamma_q}{2} + \sqrt{\left(\frac{\gamma_p - \gamma_q}{2}\right)^2 \pm K^2} \tag{5}$$

$$\gamma_2 = \frac{\gamma_p + \gamma_q}{2} - \sqrt{\left(\frac{\gamma_p - \gamma_q}{2}\right)^2 \pm K^2} \tag{6}$$

where K is the coupling factor between γ_p and γ_q.

If γ_p and γ_q represent the modes with codirectional power flow, then the upper sign $(+)$ applies in (5) and (6); but if γ_p and γ_q have contradirectional power flow, the lower sign $(-)$ applies. Note that group velocity defines the direction of power flow of a certain mode. Therefore, the slope of a certain mode in Fig. 3 defines the direction of power flow of that particular mode.

Inversely, γ_p and γ_q can be expressed in term of γ_1, γ_2, and K.

$$\gamma_p = \frac{\gamma_1 + \gamma_2}{2} + \sqrt{\left(\frac{\gamma_1 - \gamma_2}{2}\right)^2 \mp K^2} \tag{7}$$

$$\gamma_q = \frac{\gamma_1 + \gamma_2}{2} - \sqrt{\left(\frac{\gamma_1 - \gamma_2}{2}\right)^2 \mp K^2}. \tag{8}$$

In (7) and (8), if γ_1 and γ_2 have codirectional power flow, the upper sign $(-)$ applies, otherwise, the lower sign $(+)$ applies. The coupling coefficient K and the sign $(+/-)$ relate the modes before and after the coupling. Knowledge of the K value and power flow directions enables the derivation of the hypothetical modes, γ_p and γ_q, from the modes γ_1 and γ_2 (i.e., SDA data).

The resultant modal solutions γ_1 and γ_2 are the *true* electromagnetic wave solutions satisfying the boundary value problem imposed on Fig. 2. These two modes, γ_1 and γ_2, can be obtained from the full-wave SDA approach. In fact, the mode spectrum of Fig. 3 can be viewed, in a much more general sense, as not being limited to two modes. The mode γ_i represents the ith mode, where $i = 1, 2, \cdots, N$ and N is the number of modes shown in Fig. 3.

The corresponding modes to γ_1 and γ_2 *before* the coupling occurs are called the *hypothetical* modes because they do *not* satisfy the boundary value problem of the specific waveguide structure. These *hypothetical* modes with complex propagation constants, designated as γ_p and γ_q, will be shown to be very useful for explaining and modeling the three types of mode interactions summarized in Section IV.

B. *Qualitative Description of Mode-Coupling Mechanism in the Nonreciprocal Finline*

Frames (a), (b), (c), and (d) of Fig. 3 in Section IV illustrate three kinds of mode interactions existing in the nonreciprocal finline shown in Fig. 2. With the aid of two-dimensional mode-coupling theory $(N = 2)$ and the concept of hypothetical modes, described in Section V-A, the nature of mode-coupling in each case described in Section IV is investigated. Throughout the paper, the hypothetical modes γ_p and γ_q are assumed to be either a linear or an elliptical function of frequency. The determination of the hypothetical modes, γ_p and γ_q, and their

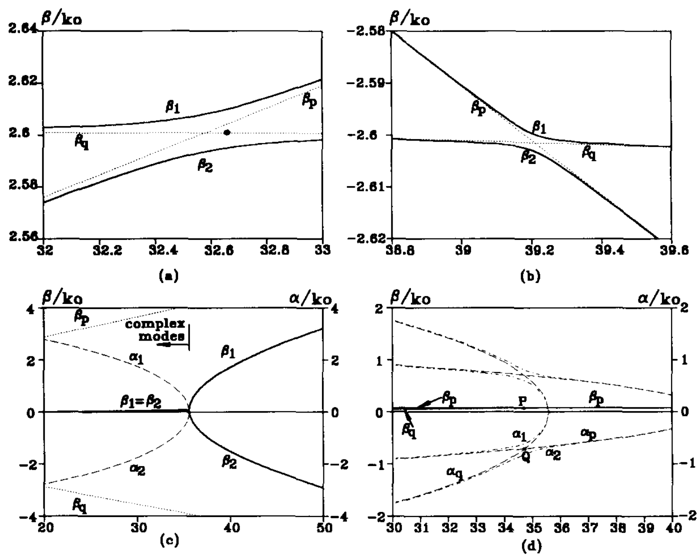

Fig. 4. Various types of mode interaction explained by mode-coupling theory. Subscripts 1 and 2 denote the true modes satisfying the boundary conditions imposed on Fig. 2. Subscripts p and q denote the hypothetical modes before the coupling occurs. All horizontal axes are the frequency axes in GHz. The solid lines and the dotted lines represent the normalized propagation constants. The dashed lines and dashed-dotted lines represent the normalized attenuation constants. (a) Mode interaction between two forward traveling waves. Solid lines: true modes; dotted lines: hypothetical modes. (b) Mode interaction between two backward traveling waves. Solid lines: true modes; dotted lines: hypothetical modes. (c) Mode interaction between a forward wave and a backward wave. Dotted lines: hypothetical modes; solid lines: real parts of γ_1 and γ_2; dashed lines: imaginary parts of γ_1 and γ_2. (d) Mode interaction between two pair of complex waves. Solid lines: real parts of hypothetical modes; dashed lines: parts of hypothetical modes; dashed-dotted lines: the corresponding γ_1 and γ_2 modes.

coupling factor K will be described in Section VI for all three kinds of mode interactions individually.

1) Mode Interaction Between a Forward (Backward) Traveling Wave and a Forward (Backward) Traveling Wave: Mode F_1 and F_2 in frame (a) of Fig. 3 are approximated by two hypothetical modes, γ_p and γ_q, which are two straight lines in the mode spectrum. The arrangement is shown in Fig. 4(a), where $\gamma_p > 0$, $\gamma_q > 0$, $\partial\gamma_p/\partial\omega > 0$, $\partial\gamma_q/\partial\omega > 0$. Thus, γ_p and γ_q represent two forward traveling waves which have codirectional power flow. To determine γ_1 and γ_2, the upper sign $(+)$ is applied in (5) and (6). Obviously, γ_1 and γ_2 are always real, and therefore no complex propagation constants can be obtained. The resultant coupled-mode solutions for γ_1 and γ_2 by applying (5) and (6) to the two assumed hypothetical modes γ_p and γ_q are also shown in Fig. 4(a).

In frame (b) of Fig. 3, modes B_2 and B_3 can also be approximated by two straight lines γ_p and γ_q as shown in Fig. 4(b). Now, $\gamma_p < 0$, $\gamma_q < 0$, $\partial\gamma_p/\partial\omega < 0$, $\partial\gamma_q/\partial\omega < 0$. Thus, γ_p and γ_q represent two backward traveling waves with codirectional power flow, which is opposite to the previous case shown in Fig. 4(a). Again, the upper sign $(+)$ is applied in (5) and (6) to determine γ_1 and γ_2. The values for γ_1 and γ_2 must also always be real and, as a consequence, there also exist no complex modes.

2) Mode Interaction Between a Forward Wave and a Backward Wave: Equations (5) and (6) indicate that the complex modes will occur when certain conditions are met. If γ_p and γ_q are two propagating modes (i.e., $\alpha = 0$), then γ_1 and γ_2 are complex modes only when the lower $(-)$ sign is applied in the square root calculation. When γ_p and γ_q are two evanescent modes (i.e., $\beta = 0$), then γ_1 and γ_2 will be complex modes only when the upper $(+)$ sign is applied to (5) and (6).

If two hypothetical modes γ_p and γ_q are assumed as shown in Fig. 4(c), a forward wave and a backward wave near the intersecting point of the two straight lines can be defined. (This will become clear in the next section.) With proper determination of the value of coupling factor K, equations (5) and (6) will yield the solutions for γ_1 and γ_2 as shown in Fig. 4(c). The two solid lines represent both the forward traveling wave and the backward traveling wave. The solid line labeled $\beta_1 = \beta_2$ shows the degenerate real parts of the complex modes and has a starting point at $\partial\beta/\partial\omega = \infty$. The dashed lines labeled α_1 or α_2 are the two imaginary parts of the complex propagation constants. These results are very similar to those reported in Fig. 3 for the same form of mode interaction.

3) Mode Interaction Between Two Complex Modes: In the next section, it will become clear that the complex propagation constants γ_1 and γ_2 have their imaginary parts on the loci of an ellipse, if γ_p and γ_q are assumed to be linear with respect to frequency. To begin, when we're interested in understanding the mode interaction between two complex modes, it is assumed that the complex modes have their complex propagation constants like those shown in Fig. 4(c). Now, the two hypothetical modes γ_p and γ_q are no longer linear functions of frequency. α_p and α_q (in dashed lines), the imaginary parts of γ_p and γ_q, represent two ellipses with long and short axes, respectively. Since β_p and β_q, the real parts of γ_p and γ_q, respectively, are two straight lines intersecting at the point P, the product of $\partial\beta_p/\partial\omega$ and $\partial\beta_q/\partial\omega$ is negative. Thus, the lower sign $(-)$ in (5) and (6) applies in this case.

Consequently, near the point P ($\alpha_p = \alpha_q$, $\beta_p = \beta_q$), the imaginary parts α_1 and α_2 of the corresponding γ_1 and γ_2 should be either higher or lower than the values of α_p (or α_q) at the intersecting point Q, where point Q and point P are at the same frequency. The results for γ_1 and γ_2 using the dashed-dotted lines for the imaginary parts are plotted for comparison with those shown in frame (d) of Fig. 3. Again, both look very similar.

By invoking the model-coupling theory and making a proper choice for the two hypothetical modes γ_p and γ_q, the entire mode spectrum shown in Fig. 3 has been explained successfully. Thus, the questions raised in Section III have been resolved, at least qualitatively.

VI. Quantitative Description of Mode-Coupling Mechanism in the Mode Spectrum of Fig. 3

The material presented in Section V explained the mode-coupling effects of various types of modes. This section shows how to determine the hypothetical modes γ_p and γ_q, and the value of the coupling factor K directly from the full-wave data shown in Fig. 3. By doing so, it is hoped that a deeper insight into the physical nature of the mode spectrum can be gained. Furthermore, if the hypothetical modes γ_p and γ_q can be obtained in a systematic and correct way, substitution of their values into equations (5) and (6), should allow comparison with the full-wave SDA solutions. If γ_p and γ_q are obtained correctly, both coupled-mode solutions and full-wave data should be inclose agreement. Since, there are mainly three distinct types of mode interactions discussed, we will investigate them separately.

A. Mode-Coupling Between Two Forward (Backward) Traveling Waves

For the case of hypothetical forward or backward traveling modes, no complex modes exist as explained in Section V-B-1. Turning to Fig. 4(a) or (b),

$$\gamma_p = \beta_p \tag{9}$$

$$\gamma_q = \beta_q \tag{10}$$

$$(\partial\beta_p/\partial\omega)\cdot(\partial\beta_q/\partial\omega) > 0 \tag{11}$$

where β_p (γ_p) and β_q (γ_q) are both real numbers and have codirectional power flow. Let

$$\Delta\beta = \beta_1 - \beta_2 . \tag{12}$$

Substituting (5) and (6) into (12), we obtain

$$\Delta\beta = 2\sqrt{\left(\frac{\beta_p - \beta_q}{2}\right)^2 + K^2} . \tag{13}$$

After some algebraic manipulations, we have

$$\left.\frac{\partial\Delta\beta}{\partial\beta_p}\right|_{\beta_p=\beta_q} = 0 \tag{14a}$$

$$\left.\frac{\partial\Delta\beta}{\partial\beta_q}\right|_{\beta_p=\beta_q} = 0 \tag{14b}$$

$$\left.\frac{\partial^2\Delta\beta}{\partial\beta_p^2}\right|_{\beta_p=\beta_q} = \frac{1}{\sqrt{K^2}} > 0 \tag{14c}$$

$$\left.\frac{\partial^2\Delta\beta}{\partial\beta_q^2}\right|_{\beta_p=\beta_q} = \frac{1}{\sqrt{K^2}} > 0 . \tag{14d}$$

Parts (a)–(d) of (14) suggest that $\Delta\beta$ has a minimum value of $2K$ when $\beta_p = \beta_q$. Turning to frame (a) of Fig. 3, an examination of the modes F_2 and F_3 shows that $\Delta\beta = \beta_1 - \beta_2$ has a minimum value. Using the data shown in frame (a) as an example, the minimum of $\Delta\beta$ occurs at 32.5 GHz, which means $\Delta\beta/ko = 2K/ko = 0.0146$. The slopes for the two straight lines β_p and β_q are approximately determined by the neighboring points on β_1 and β_2. One proper choice for β_p and β_q is as indicated in Fig. 5(a), where they are chosen as two asymptotic lines. Fig. 5(b) compares the resultant β_1 and β_2 obtained by substituting the values of β_p and β_q into equations (5) and (6) to those obtained from the SDA data. Very close agreement is obtained. The physical interpretation of Fig. 5(a) and (b) is as follows. At the point where the two hypothetical propagating modes, β_p and β_q, possessing codirectional power flow intersect, strong coupling occurs and a mode conversion (exchange) takes place. The two modes then settle to become the physical β_1 and β_2 modes.

B. Mode Coupling Between a Forward Wave and a Backward Wave: Complex Modes Occur

Assume that a forward traveling wave β_p and a backward traveling wave β_q can be approximated by two straight lines. These β_p and β_q modes are hypothetical and are defined above the frequency, f_{intsec}, the intersecting frequency of the two modes as shown in Fig. 6(a). A backward wave region, where $\beta_q \cdot (\partial\beta_q/\partial\omega) < 0$, can be defined for the hypothetical mode β_q. β_p is obviously a forward wave. Substituting the values of β_p and β_q into (5) and (6), one obtains the coupled-mode solutions γ_1 and γ_2. As shown in Fig. 6(a), a region of complex modes exists. The resultant coupled-mode solutions also exhibit a backward wave region.

From (5) and (6), the complex modes, due to mode coupling of a forward wave and a backward wave, have their imaginary parts expressed as

$$\sqrt{\left(\frac{\beta_p - \beta_q}{2}\right)^2 - K^2} = \pm j\alpha_{1 \text{ or } 2} . \tag{15}$$

Let the two straight lines representing β_p and β_q be

$$\beta_p = a \cdot f + b \tag{16}$$

$$\beta_q = c \cdot f + d \tag{17}$$

where a, b, c, d are real constants, and f is the frequency variable in gigahertz.

Substituting (16) and (17) into (15), we obtain

$$\left[f - \left(\frac{d-b}{a-c}\right)\right]^2 + \frac{\alpha^2}{\left(\frac{a-c}{2}\right)^2} = \left[\frac{K}{\frac{a-c}{2}}\right]^2 \tag{18}$$

which is an equation for an ellipse. The imaginary parts (α_1 and α_2) of the complex modes fall into the loci of an ellipse if β_p and β_q are assumed to be two linear functions of

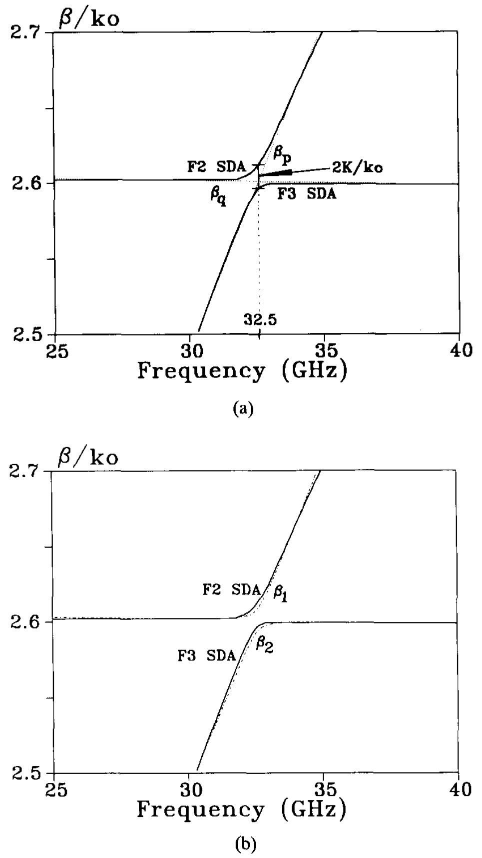

Fig. 5. Mode-coupling between two forward traveling waves. The solid lines represent the SDA data. The dotted lines represent the hypothetical modes β_p and β_q. The dashed-dotted lines represent the coupling modes β_1 and β_2. (a) Determination of the hypothetical uncoupled modes β_p and β_q from the fullwave SDA mode spectrum. F2 and F3 are two modes obtained by the SDA. $K/ko = 0.0073$. (b) Comparison of the mode spectrum obtained by SDA and that by mode-coupling using β_p and β_q obtained in (a).

frequency. The real part of the complex modes is $(\beta_p + \beta_q)/2$ derived directly from (5) and (6). The ellipse is symmetric about the frequency axis as illustrated in Fig. 6(a). When $\beta_p = \beta_q$, $|\alpha_1 - \alpha_2| = 2K$. The long axis and short axis are $K/((a-c)/2)$ and K, respectively. The ellipse is centered at point $[(d-b)/(a-c), 0]$. Once the ellipse is known, the quantities K, $(a-c)$, $(d-b)$ are readily known. We need two more equations to determine a, b, c, d. When $\alpha_{1 \text{ or } 2} = 0$ in (15), $\beta_p - \beta_q = 2K$. In Fig. 6(a) [or (b)], we may draw two vertical line segments (tangential to β_1 and β_2 curves) passing through the point where $\alpha_{1 \text{ or } 2} = 0$ or, equivalently, $\partial\beta_{1 \text{ or } 2}/\partial\omega = \infty$, either upward or downward by a distance K'. In this way, points U and D are defined as indicated in Fig. 6(a) or (b). The hypothetical modes β_p and β_q must pass through these points U and D, respectively. Substituting the two coordinates of points U and D into equations (16) and (17), respectively, we obtain another two equations. Finally, the constants a, b, c, d are solved.

The only one problem remaining is how to obtain the ellipse that approximates the region where complex modes

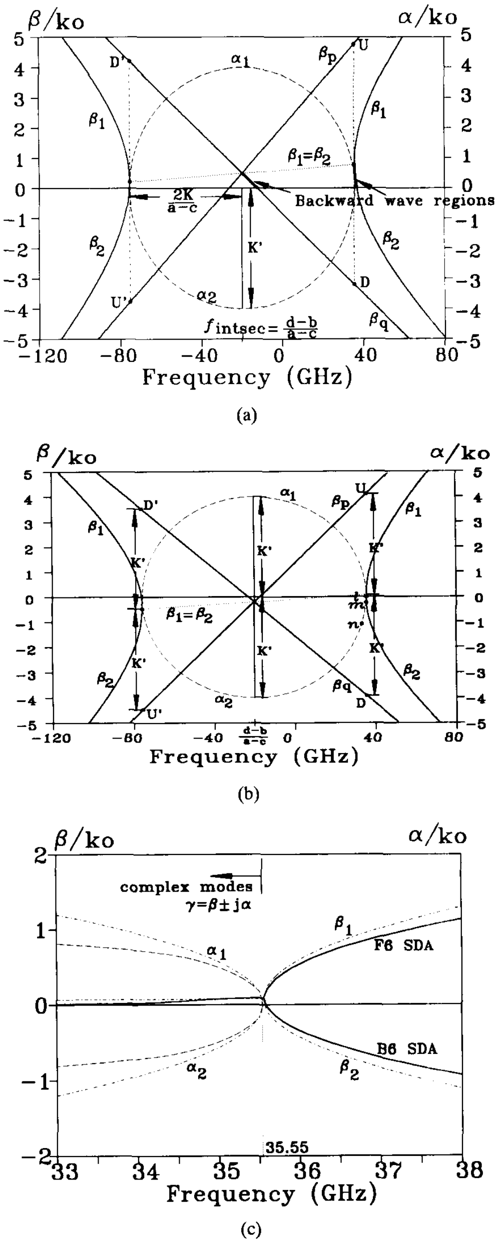

Fig. 6. Mode-coupling between a forward wave and a backward wave. The solid and dotted lines correspond with the left hand side vertical axis. The dashed lines correspond with the right hand side vertical axis. $K' = K/ko$. Synthesis of hypothetical modes β_p and β_q from the complex modes data approximated by an ellipse. (b) Determination of the ellipse obtained by the data points 1, m and n corresponding to those in frame (c) of Fig. 3. After the ellipse is known. β_p and β_q are obtained with $a/ko = 0.077$, $b/ko = 1.34$, $c/ko = -0.067$, $d/ko = -1.54$, $K/ko = 4.0$. (c) Comparison of the mode spectrum obtained by SDA and that by the model using β_p and β_q obtained in (b). the solid lines and dashed lines represent the SDA normalized propagation and attenuation constants, respectively. The dashed-dotted lines represent the corresponding coupled-mode solutions γ_1 and γ_2.

exist. Note that in the mode spectrum of Fig. 3, the regions containing complex modes can never be elliptical because the mode couplings between various complex modes occur. To avoid such influence by the existence of other complex modes nearby, Fig. 6(b) illustrates the points l, m, and n chosen for determining the ellipse using the frame (c) of Fig. 3 as an example. An ellipse can be uniquely defined by knowing three points on its loci and the even symmetry about the frequency axis. Once the ellipse is obtained, such as the one shown in Fig. 6(b), the hypothetical modes β_p and β_q can be obtained with their parameters a, b, c, d and coupling factor K, indicated in the same figure. Note that in parts (a) or (b) of Fig. 6, a small backward wave region exists.

Fig. 6(c) compares the resultant coupled-mode solutions obtained by substituting the values of β_p and β_q of Fig. 6(b) in o (5) and (6) with the full-wave SDA data near 35.55 GHz. The solid lines are for the SDA F_6–B_6 traveling wave pair and the real part of the SDA complex modes. The dashed lines are for the imaginary part of the SDA complex modes. All the dashed-dotted lines are the corresponding data obtained by the mode-coupling model. These two sets of data agree favorably.

C. Mode Coupling Between Two Complex Modes: Complex Modes Still Exist.

Using the same procedure described in the previous section, we obtain two hypothetical complex modes γ_p and γ_q corresponding to the F_7–B_7 and F_6–B_6 pairs in Fig. 3, respectively. These two hypothetical modes are *elliptical* in shape as shown in Fig. 7(a). To obtain the resultant coupled-mode solutions from γ_p and γ_q, the group velocity of the complex modes must be known. Given a pair of complex modes, say, γ_p, that propagate with the same phase velocity β_p, and the same group velocity $(\partial\beta_p/\partial\omega)^{-1}$, and that have the same magnitude but different signs for the attenuation constants, we may consider one of the complex modes carrying on exponentially decaying energy and the other an exponentially rising energy. The net sum of the total energy carried by this complex mode, γ_p, is zero [23]. In Fig. 7(a), $\gamma_p = \beta_p(7) \pm j\alpha_p(7)$ and $\gamma_q = \beta_q(6) \pm j\alpha_q(6)$. The ellipses denoted by $\pm\alpha_p(7)$ and $\pm\alpha_q(6)$ intersect at point Q. (Here, only one of the four intersecting points is shown.) Two straight lines denoted by $\beta_p(7)$ and $\beta_q(6)$ intersect at point P. Because $(\partial\beta_p/\partial\omega)\cdot(\partial\beta_q/\partial\omega) < 0$, the group velocities of the complex modes γ_p and γ_q are in opposite directions. Therefore, the lower sign $(-)$ should be applied to (5) and (6) to the resultant coupled-mode solutions γ_1 and γ_2.

When $\gamma_p = \gamma_q$, i.e., at the intersecting points of the two ellipses, (5) and (6) yield

$$\gamma_1 = \gamma_p(\text{or } \gamma_q) + jK \tag{19}$$

$$\gamma_2 = \gamma_p(\text{or } \gamma_q) - jK \tag{20}$$

$$\Delta\gamma = \gamma_1 - \gamma_2 = 2jK\,. \tag{21}$$

Accordingly, the coupling factor K can be easily obtained from the full-wave SDA data by applying (21) to the full-wave data such as that which appears in frame (d) of Fig. 3, which shows the $K/ko = 0.1$. Substituting the known value of K, the complex values of γ_p and γ_q of Fig. 7(a), which are obtained as described in the Section VI-B, into (5) and (6), we obtain the coupled-mode solutions of γ_1 and γ_2. Note that the solid and dashed lines represent the normalized complex

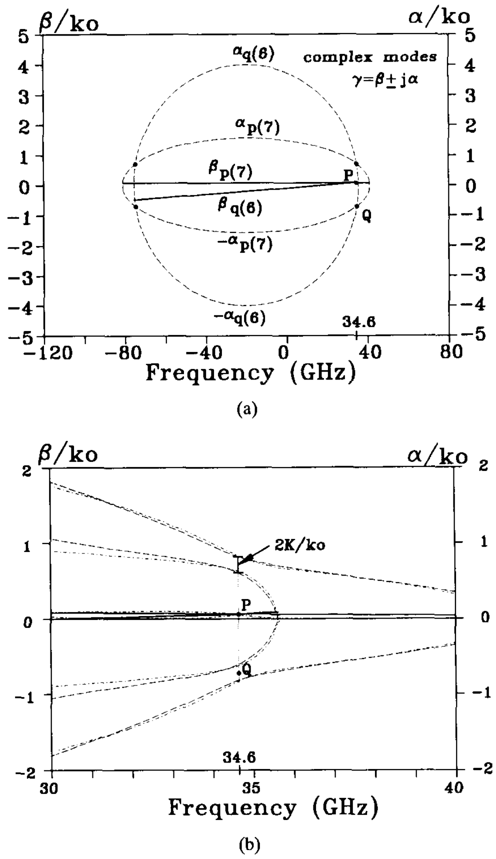

Fig. 7. Mode-coupling between two complex modes. The solid and dashed lines represent the normalized propagation constant and attenuation constant, respectively. The dashed-dotted lines represent the corresponding coupled-mode solutions γ_1 and γ_2. (a) Two hypothetical modes γ_p and γ_q obtained directly from Fig. 3 using the procedure described in Section VI-B, where the corresponding straight lines for obtaining the two ellipses are: F_6B_6: $a/ko = 0.0770$, $b/ko = 1.34$, $c/ko = -0.067$, $d/ko = -1.54$, $K/ko = 4.0$; F_7B_7: $a/ko = 0.0256$, $b/ko = 0.31$, $c/ko = 0.0256$, $d/ko = -0.712$, $K/ko = 1.57$. (b) Comparison of the mode spectrum obtained by SDA and mode-coupling (5) and (6) using γ_p and γ_q, i.e. two ellipses, obtained in (a). $K/ko = 0.1$.

propagation constants of the SDA data, while the dashed-dotted lines are for the corresponding coupled mode solutions. These two sets of data agree closely to each other. Fig. 7(b) illustrates the fact that the interaction of two pairs of complex modes may also result in the complex modes.

VII. Conclusion

In this paper, a study of the formation of complex modes using unified model-coupling theory is presented. The nonreciprocal finline, rather than the reciprocal guided-wave structure, was chosen as the vehicle for investigation so as to simplify the mode spectrum. The entire mode spectrum of Fig. 3 has been examined closely. For example, it has been shown that modal interaction between forward (or backward) traveling waves in the same direction will not produce complex modes, but that the interaction between a forward wave and a backward wave will if their propagation constants are the same, i.e., their modal spectral lines intersect. The unified mode coupling theory has been used to explain the behavior of the mode spectrum.

Beyond the qualitative description of mode-coupling effects on the mode spectrum of the nonreciprocal finline under investigation, this paper provides mathematical details on the modeling of the three types of mode interactions in the nonreciprocal finline. Good agreement between the approximated coupled-mode solutions and the full-wave SDA data for propagation constants is obtained for all three types of mode interaction. Although the physical interpretation of the hypothetical modes is not given in the paper, the authors intend to report on this subject in a separate paper.

The work performed in this paper can be extended to the study of mode-coupling effects on the reciprocal guided-wave structures without much difficulty. For example, two codirectional evanescent modes will result in a pair of complex modes that have the mathematical form of either pair 1 or pair 2 of the first type given by equations (1) and (2), respectively.

ACKNOWLEDGMENT

The authors gratefully acknowledge the constructive support from C. C. Tien and the text suggestion from J. A. Monroe. We also thank the reviewers for their comments and encouragement.

REFERENCES

[1] T. Tamir and A. A. Oliner, "Guided complex waves," *Proc. IEE*, vol. 110, no. 2, pp. 310–334, Feb. 1963.
[2] P. J. B Clarricoats and B. C. Taylor, "Evanescent and propagating modes of dielectric-loaded circular waveguide," *Proc. IEE*, vol. 111, no. 12, pp. 1951–1956, Dec. 1964.
[3] K. W. Whites and R. Mittra, "Complex and backward-wave modes in dielectrically loaded lossy circular waveguides," *Microwave Opt. Tech. Lett.*, vol. 2, no. 6, pp. 199–204, June 1989.
[4] S. B. Rayevskiy, "Some properties of complex waves in a double-layer, circular, shielded waveguide," *Radio Eng. Electron Phys.*, vol. 21, pp. 36–39, 1976.
[5] U. Crombach, "Complex waves on shielded lossless rectangular dielectric image guide," *Electron Lett.*, vol. 19, pp. 557–558, 1983.
[6] J. Strube and F. Arndt, "Rigorous hybrid-mode analysis of the transition from rectangular waveguide to shielded dielectric image guide," *IEEE Trans. Microwave Theory Tech.*, vol. MTT-33, pp. 391–401, May 1985.
[7] A. S. Omar and K. Schünemann, "The effect of complex modes at finline discontinuities," *IEEE Trans. Microwave Theory Tech.*, vol. MTT-34, pp. 1508–1514, Dec. 1986.
[8] W. X. Huang and T. Itoh, "Complex modes in lossless shielded microstrip lines," *IEEE Trans. Microwave Theory Tech.*, vol. 36, pp. 163–165, Jan. 1988.
[9] C. J. Railton and T. Rozzi, "Complex modes in boxed microstrip," *IEEE Trans. Microwave Theory Tech.*, vol. 36, pp. 865–874, May 1988.
[10] J.-T. Kuo and C.-K. C. Tzuang, "Complex modes in shielded suspended coupled microstrip lines," *IEEE Trans. Microwave Theory Tech.*, vol. 38, pp. 1278–1286, Sept. 1990.
[11] M. S. Leong, P. S. Kooi, B. Widjojo, and T. S. Yeo, "Complex modes in shielded coplanar waveguide," in *Proc. 20th EuMC*, 1990, pp. 1371–1376.
[12] J. Achkar, O. Picon, V. F. Hanna, and J. Citerne, "Analysis of symmetric and asymmetric coupled suspended striplines and some associated discontinuities," in *Proc. 20th EuMC*, 1990, pp. 537–542.
[13] A. S. Omar and K. Schünemann, "Complex and backward-wave modes in inhomogeneously and anisotropically filled waveguides," *IEEE Trans. Microwave Theory Tech.*, vol. MTT-35, pp. 268–275, Mar. 1987.
[14] M. Mrozowski and J. Mazur, "Complex waves in lossless dielectric waveguides," in *Proc. 19th EuMC*, 1989, pp. 528–533.
[15] ——, "Predicting complex waves in lossless guides," in *Proc. 20th EuMC*, 1990, pp. 487–492.
[16] ——, "Matrix theory approach to complex waves," *IEEE Trans. Microwave Theory Tech.*, vol. 40, pp. 781–785, Apr. 1992.
[17] C.-K. C. Tzuang, C.-Y. Lee, and J.-T. Kuo, "Complex modes in lossless nonreciprocal finline," *Electron Lett.*, vol. 26, no. 22, pp. 1919–1920, 1990.
[18] C. T. Tai, "Evanescent modes in a partially filled gyromagnetic rectangular wave guide," *J. Appl. Phys.*, vol. 31, pp. 220–221, 1960.
[19] M. Geshiro and T. Itoh, "Analysis of double-layered finlines containing a magnetized ferrite," *IEEE Trans. Microwave Theory Tech.*, vol. MTT-35, pp. 1377–1381, Dec. 1987.
[20] J. R. Pierce, "Coupling of modes of propagation," *J. Appl. Phys.*, vol. 25, no. 2, pp. 179–183, Feb. 1954.
[21] L. Brillouin, *Wave Propagation in Periodic Structures.* New York: Dover, 1953.
[22] C.-K. C. Tzuang and J.-M. Lin, "Mode-coupling formation of complex modes in a shielded nonreciprocal finline," in *1991 IEEE MTT-S Int. Microwave Dig.*, S-4, pp. 571–574.
[23] P. Chorney, "Power and energy relations in bidirectional waveguide," MIT Res. Lab. Tech. Rep. 396, 1961.

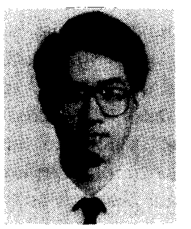

Ching-Kuang C. Tzuang (S'84–M'86–SM'92) was born in Taiwan on May 10, 1955. He received the B.S. degree in electronics engineering from the National Chiao Tung University, Hsinchu, Taiwan, in 1977 and M.S. degree from the University of California at Los Angeles in 1980.

From February 1981 to June 1984, he was with TRW, Redondo Beach, CA, working on analog and digital monolithic microwave integrated circuits. He received the Ph.D. degree in electrical engineering in 1986 from the University of Texas at Austin, where he worked on high-speed transient analyses of monolithic microwave integrated circuits. Since September 1986, he has been with the Institute of Communication Engineering, National Chiao Tung University, Hsinchu, Taiwan, R.O.C. His research activities involve the design and development of millimeter-wave and microwave active and passive circuits and the field theory analysis and design of various quasi-planar integrated circuits.

Jinq-Min Lin (S'89) was born in Taiwan on January 10, 1960. He received the B.S. degree in Physics from National Taiwan University in 1981 and the M.S. degree in Electronics from National Chiao Tung University in 1983.

Since 1984, he was with ERSO/ITRI as a researcher. He has been involved in the sub-micron project for device and TCAD development. From 1989, he has been pursuing the Ph.D. degree at the National Chiao Tung University. His research interests include microwave and millimeter-wave integrated circuit design.